

ARTICLE OPEN



Veillonellaceae family members uniquely alter the cervical metabolic microenvironment in a human three-dimensional epithelial model

Mary E. Salliss^{1,2}, Jason D. Maarsingh¹, Camryn Garza^{3,4}, Paweł Łaniewski³ and Melissa M. Herbst-Kralovetz^{1,3}✉

Bacterial vaginosis (BV) is a gynecologic disorder characterized by a shift in cervicovaginal microbiota from *Lactobacillus* spp. dominance to a polymicrobial biofilm composed of diverse anaerobes. We utilized a well-characterized human three-dimensional cervical epithelial cell model in conjunction with untargeted metabolomics and immunoproteomics analyses to determine the immunometabolic contribution of three members of the *Veillonellaceae* family: *Veillonella atypica*, *Veillonella montpellierensis* and *Megasphaera micronuciformis* at this site. We found that *Veillonella* spp. infections induced significant elevation of polyamines. *M. micronuciformis* infections significantly increased soluble inflammatory mediators, induced moderate levels of cell cytotoxicity, and accumulation of cell membrane lipids relative to *Veillonella* spp. Notably, both *V. atypica* and *V. montpellierensis* infections resulted in consumption of lactate, a key metabolite linked to gynecologic and reproductive health. Collectively our approach and data provide unique insights into the specific contributions of *Veillonellaceae* members to the pathogenesis of BV and women's health.

npj Biofilms and Microbiomes (2021)7:57; <https://doi.org/10.1038/s41522-021-00229-0>

INTRODUCTION

Human mucosae are colonized by diverse and dynamic bacterial communities that impact health and homeostasis or contribute to disease states, depending on the compositional nature of the communities¹. In the cervicovaginal microenvironment, *Lactobacillus* dominance is associated with optimal reproductive health². Lactic acid, a by-product of *Lactobacillus* fermentation, is an important metabolite in maintaining host defense and protecting the cervicovaginal mucosal epithelium from infection by sexually transmitted pathogens and opportunistic commensal bacteria³. Overgrowth of diverse anaerobic bacteria and depletion of *Lactobacillus* spp. is characteristic of bacterial vaginosis (BV) in the cervicovaginal microenvironment^{4,5}. Our group and others have developed a hypothetical model suggesting that early colonizers, such as *Gardnerella vaginalis* and *Prevotella bivia*, establish biofilm scaffolds over the cervicovaginal epithelium and exhibit low pro-inflammatory properties^{4,6}. This model proposes that as the biofilm matures, *Lactobacillus* spp. become less abundant and secondary colonizers associate with the biofilm, which results in inflammation⁴. As *Lactobacillus* spp. are depleted, BV-associated bacteria produce polyamines that result in increased pH⁴.

BV is a common and highly recurrent cervicovaginal disorder⁷. Additionally, BV has been associated with adverse obstetric and gynecologic outcomes, such as preterm birth, increased acquisition of sexually transmitted infections, and possibly gynecologic cancer^{8–13}. It is therefore imperative to better understand the pathophysiological mechanisms of BV. Key bacteria that have been the focus of BV studies thus far include *G. vaginalis*, *P. bivia*, *Sneathia amnii* and *Atopobium vaginae*, although more studies are required in order to completely elucidate contributions of the cervicovaginal microbiome to women's health^{10,14,15}. However, other vaginal commensal bacteria and BV-associated bacteria

have not been studied in detail and their roles in health or BV remain obscure. For example, members of the *Veillonellaceae* family, such as *Veillonella atypica*, *Veillonella montpellierensis* and *Megasphaera micronuciformis*, are understudied bacteria that have been isolated from the female reproductive tract^{16,17}.

V. atypica is commonly isolated from the oral cavity and has been studied extensively at this anatomical site^{18–22}. In the oral microbiome, *V. atypica* is considered a 'bridging species' that enables the colonization of middle and late colonizers to the oral plaque biofilm, with the aid of initial colonizing species, therefore *V. atypica* promotes oral biofilm development^{23–25}. In addition, *V. montpellierensis*, another *Veillonella* species, has been isolated from patients suffering from endocarditis²⁶ and acute otitis media infections²⁷. Similar to *V. atypica*, *M. micronuciformis* has also been isolated from the oral and gut microbiomes and is implicated in gastric cancer and response to chemotherapy^{28–30}.

M. micronuciformis and other *Megasphaera* spp. are typically isolated in relatively high frequency from patients with BV, along with *Atopobium*, *Leptotrichia/Sneathia*, and *Eggerthella*-like species³¹. In contrast, *Veillonella* spp. are isolated from women with and without BV and have been associated with elevated cervicovaginal pH^{31–33}. *Veillonella* spp. are commonly isolated with *Lactobacillus* spp., *G. vaginalis*, and *Peptostreptococcus* spp^{31,32}. Overall, *Veillonellaceae* family members have been isolated from women with BV^{16,17,32,34,35}, but their contributions to BV pathogenesis and biofilm formation remain understudied. Although the *Veillonella* genus is broadly reported, species-level specification is lacking in sequencing datasets^{31,32}. Therefore, we chose *V. atypica*, *V. montpellierensis*, and *M. micronuciformis* to represent *Veillonellaceae* family members present in the female genital tract to better understand their potential contributions to BV and the local microenvironment. The specific species and strains used in this study were isolated from the female genital

¹Department of Obstetrics and Gynecology, College of Medicine-Phoenix, University of Arizona, Phoenix, AZ, USA. ²Department of Biology and Biochemistry, University of Bath, Bath, UK. ³Department of Basic Medical Sciences, College of Medicine-Phoenix, University of Arizona, Phoenix, AZ, USA. ⁴Arizona State University, Tempe, AZ, USA. ✉email: mherbst1@email.arizona.edu

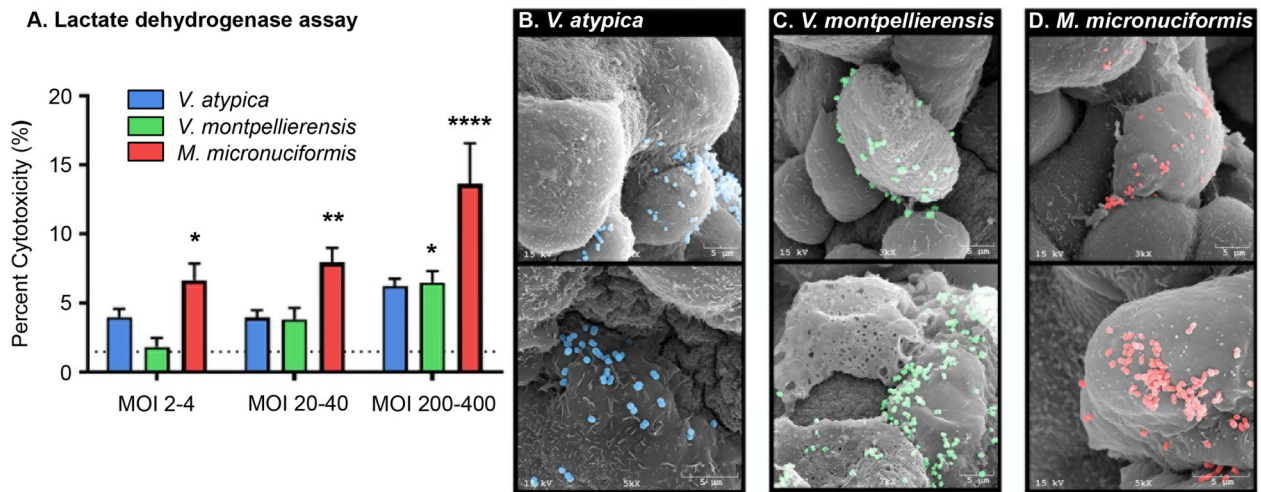


Fig. 1 *M. micronuciformis* and *V. montpellierensis* induces significant cytotoxicity in 2-D cervical cell monolayers compared to *V. atypica*. **A** LDH assay to quantify cytotoxicity in cervical epithelial monolayers. *M. micronuciformis* infections induced significant cytotoxicity to cervical epithelial monolayers at a range of MOIs from 2 to 400. *V. montpellierensis* infections induced significant cytotoxicity at the highest MOI only. Error bars designate standard deviation. Statistical differences were tested using one-way ANOVA with Dunnett's adjustment for multiple comparisons, * $P < 0.05$, ** $P < 0.005$ **** $P < 0.0001$. Scanning electron microscopy (SEM) images of **B** *V. atypica*, **C** *V. montpellierensis*, and **D** *M. micronuciformis* colonizing 3-D cervical epithelial cells. SEM images were pseudo-colored using Photoshop 19.0 CC (Adobe).

tract of women with and without BV and are available from the BEI Resources, NIAID, NIH as part of the Human Microbiome Project.

The functional impact of *V. atypica*, *V. montpellierensis*, and *M. micronuciformis* on host response mechanisms in the human cervix, which can contribute to poor gynecologic and reproductive outcomes, has not been previously investigated. Therefore, we aimed to evaluate the immunometabolic contributions of *V. atypica*, *V. montpellierensis*, and *M. micronuciformis* in the cervical microenvironment to better understand the role of these species in BV and other sequelae. To achieve this, we used a robust and extensively characterized human three-dimensional (3-D) cervical epithelial cell model for the study of host-microbe interactions and infected the model with clinical isolates of *Veillonellaceae* family members, coupled with untargeted global metabolomics and immunoproteomics approaches. We chose to use a 3-D cervical cell model due to the clinical relevance of studying BV-associated bacteria in the context of the cervix as it relates to human papillomavirus (HPV), HIV, *Chlamydia trachomatis*, and *Neisseria gonorrhoeae* infections^{36–39}. Additionally, *M. micronuciformis* has been isolated from women suffering from preterm birth^{40–42}. *Veillonella* spp. have been implicated in secondary bacteremia in a pregnant woman, but the potential for *Veillonella* spp. to participate as opportunistic pathogens in the female reproductive tract is understudied⁴³.

The 3-D cervical model is a robust system to study host-microbe interactions, as it accurately resembles ultrastructural features of the cervical tissue in vivo, such as apical and basal differentiation, tight junctions, microvilli, and more organotypic surfaces for the colonizing bacteria, and has been shown to recapitulate clinical findings^{15,44–47}. Herein, we applied a reductionist approach and infected the 3-D cervical model with single bacterial species to determine the individual contributions of these bacteria to the cervicovaginal microbiome that are currently lacking. This knowledge is essential to inform future experiments that involve polymicrobial infections^{44–47}.

RESULTS

M. micronuciformis infections induce moderate cytotoxicity to cervical epithelial cells

First, we screened cervical epithelial monolayers for cytotoxicity following infection with *V. atypica*, *V. montpellierensis*, and

M. micronuciformis at multiplicities of infection (MOIs) ranging from 2 to 400. We found that *M. micronuciformis* induced significant cytotoxicity at all tested MOIs (6.65%, 7.96%, and 13.63%) to cervical epithelial cell monolayers ($P = 0.0291$, $P = 0.0041$, and $P < 0.0001$ respectively); however, cervical epithelial cytotoxicity induced by *M. micronuciformis* infections was still modest at the highest MOI. *V. montpellierensis* infections induced cytotoxicity to cervical epithelial monolayers at only the highest MOI tested (6.50%, $P = 0.0359$). *V. montpellierensis* infections did not induce significant epithelial cytotoxicity at MOIs 2–4 and 20–40 (1.84%, 3.85%, respectively). Percentage cytotoxicity of *V. atypica* infections resulted in similar epithelial cytotoxicity at all tested MOIs (3.99%, 3.94%, and 6.23%) (Fig. 1A). Since *Veillonella* and *Megasphaera* spp. are predicted to harbor genes encoding lactate dehydrogenase (LDH)^{48,49}, we also assessed the cytotoxicity using crystal violet staining (Supplementary Fig. 1). These results were consistent with LDH activity data with respect to cell viability measurements, indicating that potential bacterial LDH activity did not impact these data.

Next, we infected human 3-D cervical models with *V. atypica*, *V. montpellierensis*, and *M. micronuciformis* and confirmed colonization of the 3-D aggregates by SEM (Fig. 1B–D). Generally, *V. atypica*, *V. montpellierensis*, and *M. micronuciformis* sparsely colonized the 3-D cervical epithelial cells with occasional small clusters of bacteria co-localizing together on cervical cells. *V. montpellierensis* appeared to mostly colonize the surface of dead cells as visualized by SEM. *M. micronuciformis* also tended to sparsely cluster with other bacteria on cervical epithelial cell surfaces.

Infection with *M. micronuciformis* induces significantly elevated 3-D cervical cell pro-inflammatory responses while *V. atypica* significantly decreases the expression of specific epithelial barrier targets

Since BV is accompanied by mild genital inflammation, remodeling of the extracellular matrix, and cell lysis^{46,50}, we examined the secretion of cytokines (IL-1 α , IL-1 β , IL-1RA, IL-6, and TNF- α), chemokines (fractalkine, IL-8, IP-10, MCP-1, MCP-3, MIP-1 β , and RANTES), growth factors (PDGF-AA, TGF- α , and VEGF), apoptosis-related proteins (MIF, TRAIL, sFasL), mucins (CEA and CA125) and matrix metalloproteinases (MMP-1, MMP-7, MMP-9, MMP-10) in

A. Immunoproteomics analysis

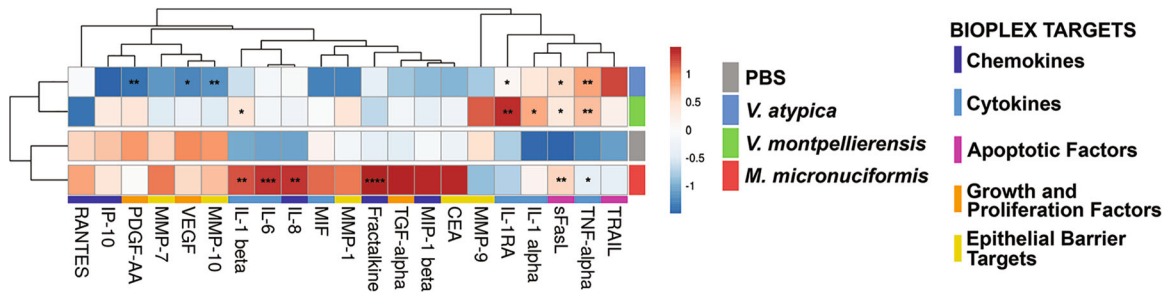


Fig. 2 *M. micronuciformis* infections induced greater secretion of pro-inflammatory cytokines and chemokines, but *V. atypica* infections significantly decreased the culture concentration of some barrier targets. **A** Hierarchical clustering analysis (HCA) of immunoproteomics data from human 3-D cervical epithelial cells infected with *V. atypica*, *V. montpellierensis*, or *M. micronuciformis* under anaerobic conditions for 24 h. Statistical significance was determined using one-way ANOVA with Dunnett's adjustment for multiple comparisons relative to PBS; * $P < 0.05$, ** $P < 0.01$, *** $P < 0.001$, **** $P < 0.0001$. Color labels for each bacterial infection are observed to the right of the HCA and are as follows: PBS (gray), *V. atypica* (blue), *V. montpellierensis* (green), and *M. micronuciformis* (red). Protein targets (bottom of HCA) were color-coded in order to visualize clustering patterns of the protein targets: apoptotic factors (pink), epithelial barrier targets (yellow), growth and proliferation factors (orange), chemokines (dark blue), and cytokine (light blue). Individual concentrations can be visualized on graphs in the supplementary information (Supplementary Figs. 2–4).

the 3-D cervical epithelial cell models infected with *V. atypica*, *V. montpellierensis* or *M. micronuciformis* at MOI 20–40 for 24 h. We analyzed 3-D cervical cell culture supernatants using cytometric bead arrays to quantify the host response to infection with these bacteria. *V. atypica* induced significant elevation of sFasL ($P = 0.0202$), IL-1RA ($P = 0.0498$), TNF- α ($P = 0.0152$), and significantly decreased secretion of PDGF-AA ($P = 0.0083$), VEGF ($P = 0.0245$), and MMP-10 ($P = 0.0064$). Infection with *V. montpellierensis* induced significant elevation of sFasL ($P = 0.0250$) and IL-1 α ($P = 0.0137$), IL-1RA ($P = 0.0095$), TNF- α ($P < 0.0001$), IL-1 β ($P = 0.0470$). *M. micronuciformis* significantly induced secretion of sFasL ($P = 0.0065$), TNF- α ($P = 0.0056$), IL-1 β ($P = 0.0012$), IL-6 ($P = 0.0004$), fractalkine ($P < 0.0001$), and IL-8 ($P = 0.0012$) (Fig. 2A, Supplementary Figs 2–4).

We utilized hierarchical clustering analysis for evaluating immune response profiles for each bacterial infection. *V. atypica* and *V. montpellierensis* exhibited similar immunoproteomic profiles and clustered separately from *M. micronuciformis* or PBS controls (Fig. 2A). Overall, *M. micronuciformis* induced the secretion of pro-inflammatory cytokines and chemokines to a greater extent compared to *V. atypica* and *V. montpellierensis* and PBS controls. Infection with *V. atypica* resulted in a decrease in the concentration of PDGF-AA, VEGF, and MMP-10.

Untargeted global metabolomics analysis revealed similar metabolic profiles between *V. atypica* and *V. montpellierensis* that are distinct from *M. micronuciformis*

We next sought to define how *V. atypica*, *V. montpellierensis*, and *M. micronuciformis* alter the metabolomic landscape of 3-D cervical cell culture supernatants using high-throughput global untargeted metabolomics. Principal component analysis (PCA) of global metabolomic profiles (Fig. 3A) revealed that *V. atypica* and *V. montpellierensis* metabolomes cluster together, whereas *M. micronuciformis* and PBS controls tended to cluster together and separately from both *Veillonella* groups. Relative to PBS controls, PC1 (36.8% of explained variance) scores were significantly different between *V. atypica* and *V. montpellierensis* ($P < 0.0001$). No significant differences were found between PBS controls and any strain tested with respect to PC2 (19.2% of explained variance) scores.

We then applied non-parametric correlation analyses (Fig. 3B) to visualize the clustering of biological replicates. We observed that metabolomic profiles of *V. atypica* and *V. montpellierensis* correlated well with each other; however, the cluster analysis

failed to group individual replicates of the same species, therefore suggesting highly similar metabolic profiles among the two *Veillonella* spp. While in the same parent cluster, the metabolomic profiles for *M. micronuciformis* and PBS controls mostly separated from each other. PBS controls correlated well between individual replicates, with the exception of one infection replicate with *M. micronuciformis*. Overall, the correlation analysis supported the PCA results.

We further investigated differences in metabolic profiles of *V. atypica*, *V. montpellierensis*, and *M. micronuciformis* infections by comparing the super-pathways of significantly changed metabolites relative to PBS controls (Fig. 3C). The composition of metabolic super-pathways for *M. micronuciformis* was significantly different from that of *V. atypica* ($P = 0.0016$) and *V. montpellierensis* ($P < 0.0027$). The super-pathways that were most different between *V. atypica*, *V. montpellierensis*, and *M. micronuciformis* were lipid (8.70%, 16.33%, and 38.1% respectively) and amino acid (47.83%, 52.04%, and 31.75% respectively).

Veillonella spp. and *M. micronuciformis* infections result in enrichment in amino acids and lipids, respectively

Next, we performed metabolite pathway enrichment analysis using MetaboAnalyst (Fig. 3C). Metabolomic profiles from infection with *V. atypica* and *V. montpellierensis* were significantly enriched in metabolic pathways corresponding to arginine and proline ($P = 0.0151$ and $P = 0.0076$, respectively), butanoate ($P = 0.0032$ and $P = 0.0060$, respectively), cysteine and methionine ($P = 0.0041$ and $P = 0.0014$, respectively), histidine ($P = 0.0106$ and $P = 0.0089$, respectively) and glutathione ($P = 0.0117$ and $P = 0.0061$, respectively) metabolism (Fig. 4D). Infection with *V. montpellierensis* also significantly enriched four additional pathways corresponding to amino sugar and nucleotide sugar ($P = 0.0199$), riboflavin ($P = 0.0425$), tryptophan ($P = 0.0394$), and glycerolipid ($P = 0.0497$) metabolism.

Infection with *M. micronuciformis* modulated five significantly enriched pathways, including tyrosine metabolism ($P = 0.0493$), sulfate metabolism ($P = 0.0309$), steroid biosynthesis ($P = 0.0159$), steroid hormone biosynthesis ($P = 0.0189$), and primary bile acid synthesis ($P = 0.01520$). These pathways were unique to infection with *M. micronuciformis* relative to *V. atypica* or *V. montpellierensis* infections (Supplementary Figure 5).

We found variations in lipid metabolism both in our metabolite composition analysis (Fig. 3C) and enrichment analysis (Fig. 4D) for *V. montpellierensis* and *M. micronuciformis* infections. Significantly

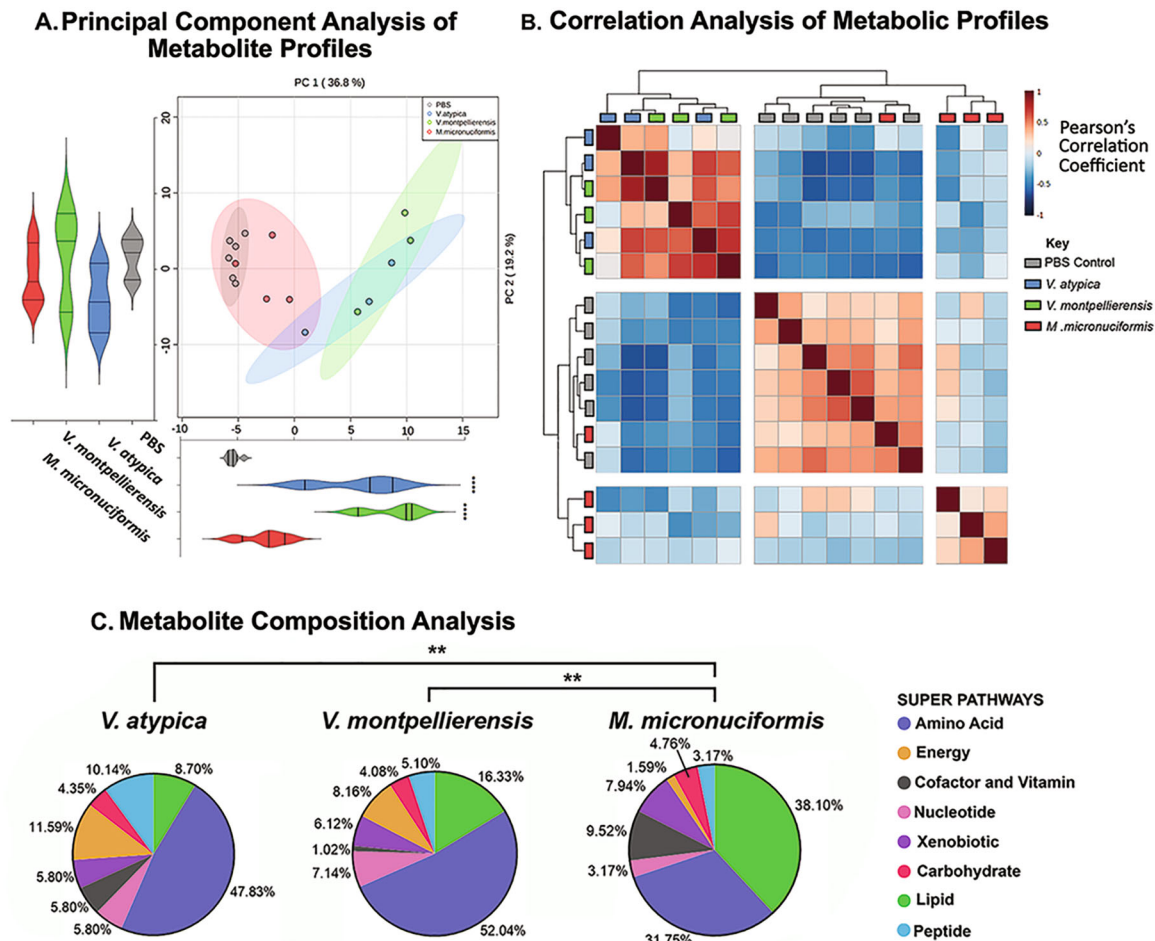


Fig. 3 Both *Veillonella* species are metabolically similar to each other and distinct from PBS controls, while *M. micronuciformis* shares similar metabolic profiles with PBS controls. Global metabolic analysis of cell culture supernatants from human 3-D cervical epithelial cells infected with *V. atypica*, *V. montpellierensis*, or *M. micronuciformis* under anaerobic conditions for 24 h. **A** Principal component analysis (PCA) shading indicates the 95% confidence interval and **B** Pearson's correlation analysis of metabolomics data displays how sample metabolic profiles relate to each other. Blue and red coloring indicate negative and positive correlations between samples, respectively. **C** Pie charts of significantly changed metabolites. The percentage of metabolites that were approached significance ($P < 0.1$) within each super pathway are labeled next to each slice (the total number of significantly altered metabolites for *V. atypica*, *V. montpellierensis*, and *M. micronuciformis* were 69, 98, 63 respectively). PCA significance (**A**) was tested by one-way ANOVA and Dunnett's adjustment for multiple comparisons relative to PBS; **** $P < 0.0001$. The significance of differences between metabolite compositions (**C**) was tested using a chi-squared test of trends; ** $P < 0.01$.

enriched pathways corresponding to lipid metabolism included glycerolipid metabolism and steroid and steroid hormone biosynthesis as modulated by *V. montpellierensis* and *M. micronuciformis*, respectively. Metabolic pathways corresponding to lipid metabolism were not significantly enriched by infection with *V. atypica*, therefore suggesting *V. montpellierensis* and *M. micronuciformis* influence species-specific lipid metabolic products following infection of 3-D cervical cells.

***V. atypica* and *V. montpellierensis* infections resulted in significant elevation of polyamines and depletion of lactate, whereas glycerolipids were significantly elevated with *M. micronuciformis* infections**

Finally, we assessed specific metabolites that were significantly elevated or depleted in response to *V. atypica*, *V. montpellierensis*, and *M. micronuciformis* infections relative to PBS controls. Culture supernatants from human 3-D cervical cells infected with *V. atypica* and *V. montpellierensis* significantly accumulated polyamines, such as cadaverine ($P = 0.0159$ and $P = 0.0037$), putrescine ($P = 0.0155$ and $P = 0.00485$), agmatine ($P = 0.0444$ and $P = 0.0170$), and histamine ($P = 0.0331$ and $P = 0.0452$) (Fig. 5B).

Additionally, *V. montpellierensis* infections induced accumulation of spermidine ($P = 0.0363$) and *N*-acetyl-cadaverine ($P = 0.00207$). Metabolites involved in polyamine production were significantly depleted by infection with *V. atypica* and *V. montpellierensis*, including argininosuccinate ($P = 0.0319$ and $P = 0.0179$), ornithine ($P = 0.0108$ and $P = 0.00140$), and 5-methylthioadenosine ($P = 0.0216$ and $P = 0.0266$). The cervicovaginal pH-lowering metabolite, lactate, was also significantly depleted by infection with *V. atypica* and *V. montpellierensis* ($P = 0.0162$ and $P < 0.0001$, respectively).

Culture supernatants from 3-D cervical cells infected with *M. micronuciformis* accumulated glycolipids and sphingolipids (Fig. 5 and Supplementary Data 1). The short-chain fatty acid (SCFA) 2-hydroxybutyrate/2-hydroxyisobutyrate was also significantly elevated by infection with *V. atypica*, *V. montpellierensis*, and *M. micronuciformis* ($P = 0.0344$, $P = 0.0006$, and $P = 0.0253$, respectively). Specific glycerophospholipid and sphingolipid species were significantly elevated following *M. micronuciformis* infections including: 1,2-dipalmitoyl-GPC (16:0/16:0) ($P = 0.0188$), *N*-palmitoyl-sphingosine (d18:1/16:0) ($P = 0.0363$), cholesterol ($P = 0.0465$) and 1-stearoyl-2-oleoyl-GPC (18:0/18:1) ($P = 0.0470$). 1-(1-enyl-

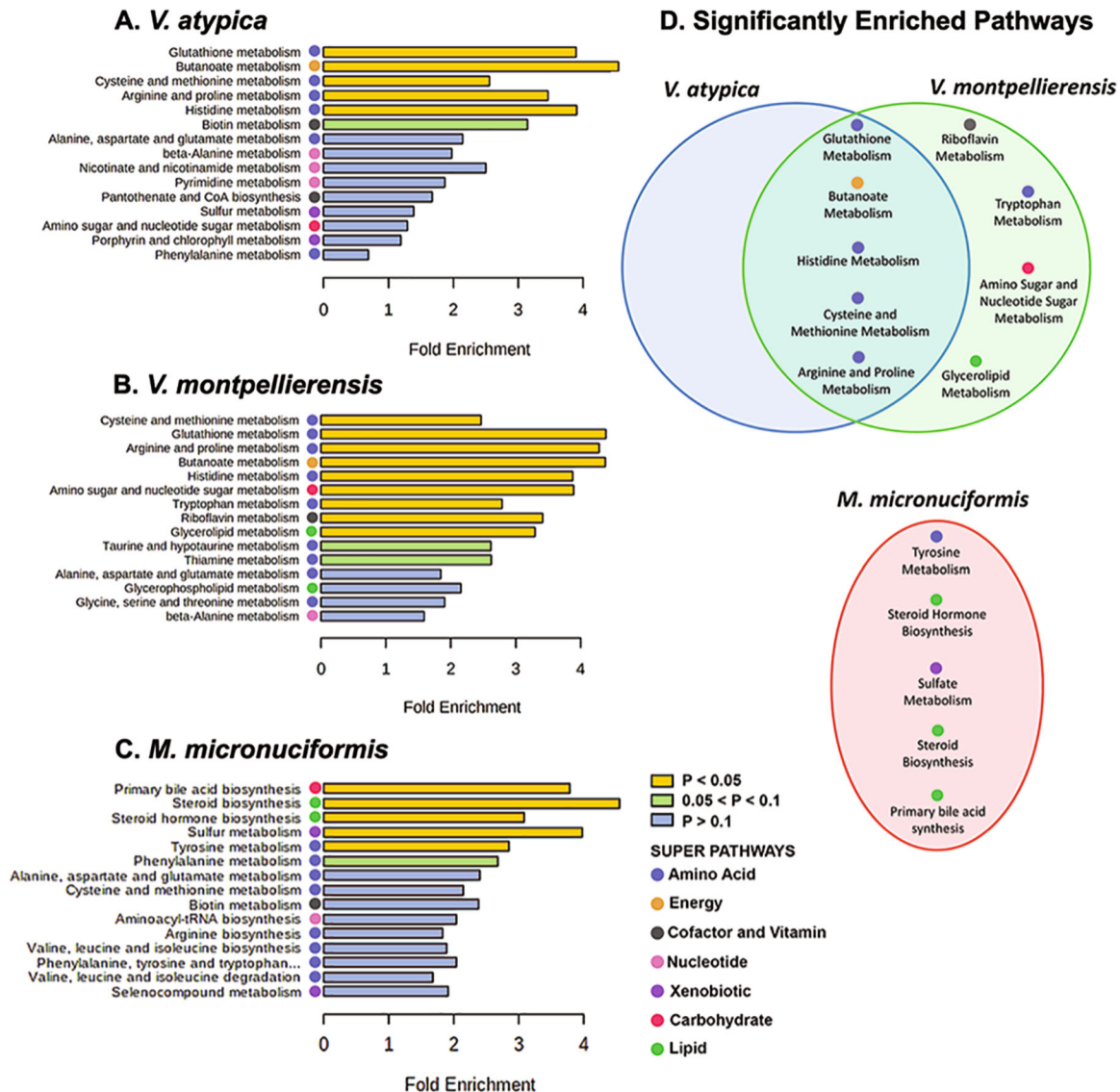


Fig. 4 *V. atypica* and *V. montpellierensis* share overlapping enrichment of metabolic pathways belonging to amino acid metabolism that are distinct from *M. micronuciformis*. Metabolite pathway enrichment analysis of human 3-D cervical epithelial cells infected with **A** *V. atypica* (Supplementary Fig. 3), **B** *V. montpellierensis* (Supplementary Fig. 4), and **C** *M. micronuciformis* (Supplementary Fig. 5), under anaerobic conditions for 24 h. **D** Comparison of significantly enriched metabolic pathways between infections. Color bars indicate significance, yellow represents pathways that are significantly enriched ($P < 0.05$), green indicates pathways that approach statistical significance ($0.05 < P < 0.1$), and blue indicates pathways that were not significantly enriched ($P > 0.1$). The super pathway that a particular sub-pathway belongs to is indicated with colored circles.

palmitoyl)-2-oleoyl-GPE (P-16:0/18:1) was significantly elevated by infection with *V. atypica*, *V. montpellierensis*, and *M. micronuciformis* ($P = 0.0438$, $P = 0.0292$, and $P = 0.0426$, respectively). In *V. montpellierensis* and *M. micronuciformis* infections, 1-palmitoyl-2-oleoyl-GPE (16:0/18:1) was significantly elevated ($P = 0.00969$ and $P = 0.0209$, respectively). Two glycerolipids were significantly elevated by infection with *V. montpellierensis*: glycerol-3-phosphate ($P = 0.0405$) and 1-stearoyl-2-oleoyl-GPE (18:0/18:1) ($P = 0.0491$). Overall, *M. micronuciformis* infections significantly elevated the glycerophospholipids and sphingolipids to a greater magnitude relative to *V. atypica* and *V. montpellierensis* infections.

In addition, 2-hydroxyglutarate (an oncometabolite) was significantly elevated during infection with *V. atypica* and *V. montpellierensis* ($P = 0.0308$ and $P = 0.0052$, respectively), with *V. atypica* infections ($P = 0.0268$), and betaine was altered with *V. montpellierensis* infections ($P = 0.0102$). Urate (an HPV-associated

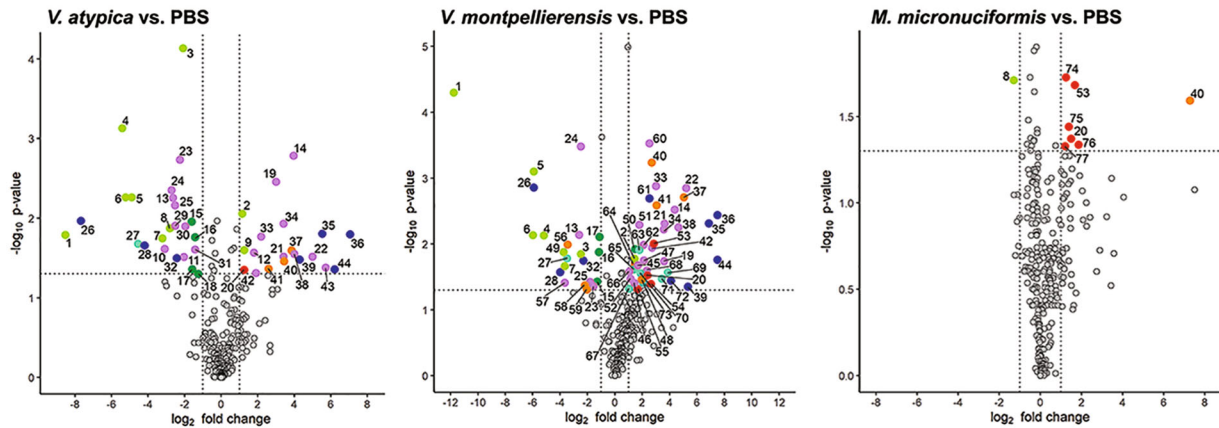
metabolite)⁵¹ was significantly increased with *V. atypica* infections ($P = 0.0244$).

Overall, infection of 3-D cervical epithelial cells with *V. atypica* or *V. montpellierensis* induced significant elevation of metabolites associated with a higher cervicovaginal pH and amine odor, combined with depletion of metabolites involved with polyamine biosynthesis. *M. micronuciformis* infections significantly elevated glycerolipids and sphingolipids that are potentially indicative of cervical epithelial cell cytotoxicity (Fig. 5).

DISCUSSION

Members of the *Veillonellaceae* family, *V. atypica*, *V. montpellierensis*, and *M. micronuciformis* have been isolated from women with BV and healthy women^{2,16,17,31,32,34,40}; however, the mechanisms employed by these bacteria that relate to BV pathogenesis and

A. Volcano plot analysis



B. Significantly altered metabolites

TCA/Krebs Cycle

No.	Metabolites	Associated with	Altered by	Ref.
1	Lactate	⊗	⊕	[53,75]
3	Succinate	⊗	⊕	[58,75]
4	Malate	⊗	⊕	[58]
5	Aconitate [cis or trans]	⊗	⊕	[58]
6	Citrate	⊗	⊕	[58]
7	Fumarate	⊗	⊕	[58,44]
8	Nicotinamide	⊗	⊕	[58]
49	α-ketoglutarate	⊗	⊕	[58,75]
2	Phosphoenolpyruvate	⊗	⊕	[58]
9	NAD+	⊗	⊕	[58,75]

Polyamine Synthesis

No.	Metabolites	Associated with	Altered by	Ref.
26	Ornithine	⊕	⊕	[75]
28	5-methylthioadenosine (MTA)	⊕	⊕	[75]
32	Argininosuccinate	⊕	⊕	[75]
35	Putrescine	⊕	⊕	[76]
36	Cadaverine	⊕	⊕	[75]
39	Histamine	⊕	⊕	[75]
44	Agmatine	⊕	⊕	[75]
61	N-acetyl-cadaverine	⊕	⊕	[7,44]
72	Spermidine	⊕	⊕	[7]

Acetylated amino acids

No.	Metabolites	Associated with	Altered by	Ref.
27	N-acetylaspartate (NAA)	?	⊕	
63	N-acetylthreonine	?	⊕	
65	N-acetylglutamine	?	⊕	
67	N-acetyserine	?	⊕	
69	N-acetylcysteine	?	⊕	
70	N-acetylvaline	?	⊕	
71	N-acetylarginine	?	⊕	
73	N-acetyl-leucine	?	⊕	

METABOLITES ASSOCIATED WITH...

⊗	Energy Metabolism	⊕	HPV (+) infection
⊗	Amine Odour	⊕	Epithelial Barrier Function
⊕	Vaginal Discharge	⊕	Polyamine Production

Short chain fatty acids (SCFAs)

No.	Metabolites	Associated with	Altered by	Ref.
58	4-methyl-2-oxopentanoate	?	⊕	
59	3-methyl-2-oxovalerate	?	⊕	
56	3-methyl-2-oxobuturate	?	⊕	
37	2-hydroxy-4-(methylthio)butanoic acid	⊕	?	
40	2-hydroxybutyrate/2-hydroxyisobutyrate	⊕	?	[44]
41	α-hydroxyisocaproate	⊕	?	
48	2,3-dihydroxyisovalerate	⊕	?	
64	α-hydroxyisovalerate	⊕	?	[44]

Glycerolipids and Sphingolipids

No.	Metabolites	Associated with	Altered by	Ref.
20	1-(1-enyl-palmitoyl)-2-oleoyl-GPE (P-16:0/18:1)	⊕	?	[44,75]
53	1-palmitoyl-2-oleoyl-GPE (16:0/18:1)	⊕	?	[44,75]
54	Glycerol-3-phosphate	⊕	?	
55	1-stearoyl-2-oleoyl-GPE (18:0/18:1)	⊕	?	[44,75]
74	1,2-dipalmitoyl-GPC (16:0/16:0)	⊕	?	[44,75]
75	N-palmitoyl-sphingosine (d18:1/16:0)	⊕	?	[44,75]
76	cholesterol	⊕	?	
77	1-stearoyl-2-oleoyl-GPC (18:0/18:1)	⊕	?	[44,75]

Dipeptides

No.	Metabolites	Associated with	Altered by	Ref.
15	γ-glutamylisoleucine	⊗	⊕	[75]
16	Glycylvaline	⊗	⊕	[75]
17	Phenylalanylglycine	⊗	⊕	[75]
18	Glycylleucine	⊗	⊕	[75]
50	γ-glutamylmethionine	⊗	⊕	[75]

Miscellaneous Metabolites

No.	Metabolites	Associated with	Altered by	Ref.
10	Urate	⊕	⊕	[44]
11	Allantoin	?	⊕	
13	Tartarate	⊗	⊕	[44]
23	1-carboxyethylvaline	?	⊕	
24	Cysteinylglycine	?	⊕	
25	1-carboxyethylleucine	?	⊕	
29	1-carboxyethylphenylalanine	?	⊕	
30	Imidazole propionate	?	⊕	
31	Cysteine-glutathione disulfide	?	⊕	
57	Glutamate	H ⁺ /OH ⁻	⊕	[75]
12	Adenosine	⊕	⊕	[44]
14	2-isopropylmalate	?	⊕	
19	Propionylcarnitine	?	⊕	
21	2-hydroxyglutarate	⊗	⊕	[77]
22	Methylmalonate	?	⊕	
33	3-(4-hydroxyphenyl) lactate	?	⊕	
34	Imidazole lactate	?	⊕	
38	N-propionylmethionine	?	⊕	
42	Indolelactate	?	⊕	
43	Phenylpyruvate	?	⊕	
45	Mannitol/sorbitol	?	⊕	
46	N-acetylglucosamine-6-phosphate	?	⊕	
47	β-guanidinopropanoate	?	⊕	
51	β-alanine	?	⊕	
52	Uridine	?	⊕	
60	N-formylmethionine	?	⊕	
62	Betaine	⊕	⊕	[7,44]
66	Oxidindolalanine	?	⊕	
68	4-hydroxyphenylpyruvate	?	⊕	

Significantly Decreased Metabolites, due to bacterial infections

Significantly Increased Metabolites, due to bacterial infections

⊗	Energy Metabolism	⊕	HPV (+) infection	⊗	Oncometabolites/Associated with Cancer	H ⁺ /OH ⁻	Elevated Cervicovaginal pH	⊕	<i>V. atypica</i>
⊗	Amine Odour	⊕	Epithelial Barrier Function	?	Understudied Metabolites	⊕	Cell Death/Cytotoxicity	⊕	<i>V. montpellierensis</i>
⊕	Vaginal Discharge	⊕	Polyamine Production	⊕	Cervicovaginal health	⊕	Cervicovaginal Inflammation	⊕	<i>M. microneuciformis</i>

Fig. 5 Metabolites associated with elevated cervicovaginal pH were significantly altered by *V. atypica* and *V. montpellierensis*, whereas metabolites associated with cell death were significantly accumulated with *M. microneuciformis* infections. Human 3-D cervical epithelial cells were infected with *V. atypica*, *V. montpellierensis*, or *M. microneuciformis* under anaerobic conditions for 24 h. **A** Volcano plots of *V. atypica*, *V. montpellierensis* and *M. microneuciformis* metabolic profiles. The x axis represents the log₂ fold change values of metabolite scaled intensity values between the infectious treatment and PBS control. The y axis represents the $-\log_{10}(P)$ value of differential metabolite abundance between infectious treatment and PBS controls (paired two-tailed Student's *t*-test). **B** Significantly different metabolites ($P < 0.05$) with a fold-change < -2 or > 2 are colored by super pathway. Symbols indicate how the metabolite may impact BV pathogenesis. See Supplementary Data 1 for specific *P*-values, *q*-values, and mean fold changes of all measured metabolites.

other gynecologic and obstetric sequelae are unknown. In this study, we aimed to elucidate the metabolic and inflammatory contributions of *V. atypica*, *V. montpellierensis*, and *M. microneuciformis* to reveal the function of these organisms in the cervical microenvironment.

To our knowledge, colonization of human organotypic genital epithelial cells by *V. atypica*, *V. montpellierensis*, or *M. microneuciformis* in vitro has not been previously demonstrated and visualized. Using our human 3-D cervical epithelial cell model, we demonstrated that *V. atypica*, *V. montpellierensis*, and

M. micronuciformis are capable of colonizing cervical epithelial cell surfaces (Fig. 1B–D). Our human 3-D cervical epithelial cell model expresses mucins and TLRs and other physiological relevant features of parental human cervical tissue that may enhance colonization of bacteria compared to traditional 2-D monolayer cultures^{46,52}.

The cytotoxic potential of *Veillonellaceae* members in the cervical epithelium has not been thoroughly explored. One study tested an unnamed *Veillonella* spp. on vaginal epithelial cell monolayers and found no evidence for cell death, though this was not quantified⁵³. Our data suggest that *M. micronuciformis* induces moderate cytotoxicity, whereas *V. atypica* and *V. montpellierensis* do not significantly contribute to cervical epithelial cell death (Fig. 1). In this capacity, *M. micronuciformis* may therefore contribute to the breakdown of epithelial barrier function, in accordance with other BV-associated bacteria⁴.

To our knowledge, the pro-inflammatory host response to cervical infection with *M. micronuciformis* has not been previously examined in vitro, though another species under the *Megasphaera* genus (*Megasphaera elsdenii*) has been investigated⁵⁴. In this study, dendritic cells elevated secretion of IL-1 β , IL-6, IL-8, IL-12p40, and TNF- α in response to infection with *M. elsdenii*⁵⁴. Additionally, *M. micronuciformis* was associated with genital inflammation as measured from cervicovaginal fluid in a cohort of South African adolescent females⁵⁵. However, no studies have identified the immune response to *V. atypica* and *V. montpellierensis* in the cervicovaginal context. Our results suggest that *M. micronuciformis* induced a robust human 3-D cervical epithelial cell pro-inflammatory response marked by upregulated secretion of pro-inflammatory cytokines and chemokines, whereas both *V. atypica* and *V. montpellierensis* induced relatively fewer pro-inflammatory mediators (Fig. 2A). We hypothesize that *M. micronuciformis* is more pro-inflammatory than *V. atypica* or *V. montpellierensis* in the cervicovaginal environment, which is in the accordance with the literature, although more studies are required that investigate *Veillonella* spp. in the cervicovaginal environment.

SCFA production is a metabolic hallmark of BV as demonstrated in clinical and in vitro studies^{56–58} and have been linked to increased secretion of pro-inflammatory mediators⁵⁹. We observed a higher accumulation of *N*-palmitoyl-sphingosine in response to infection with *M. micronuciformis* compared to *V. atypica* or *V. montpellierensis*, and is associated with inflammation⁶⁰. *Veillonella* spp. and *M. micronuciformis* also induced upregulated secretion of several pro-inflammatory mediators from the 3-D cervical model, which is consistent with the literature and SCFA elevation⁵⁹ and could indicate that SCFAs are both a hallmark of BV and indicators of cervical inflammation.

Histamine, a key metabolite involved in local host responses, was significantly accumulated by infection with *V. atypica* and *V. montpellierensis*. Other studies have found that histamine can decrease the expression of tight junctional proteins (ZO-1 in nasal epithelial cells and E-cadherin in epithelial pulmonary cells)⁶¹. Therefore, an increase in histamine may increase epithelial permeability, although this would need to be tested in the context of the cervicovaginal epithelium to confirm the role of histamine in barrier function within the cervicovaginal mucosa.

Our metabolomics analyses revealed changes in the lipid metabolism following infections with *Veillonellaceae* family members. Infection with *M. micronuciformis* induced significant accumulation in glycerolipids and sphingolipids (Fig. 5). We also observed a significant accumulation in glycerolipids and cholesterol during human 3-D cervical cell infections with *V. atypica*, *V. montpellierensis*, and *M. micronuciformis*. To date, there are few studies that have reported an association with elevated glycerolipids and cell death, but sphingolipids have been related to cell death⁶². In our previous clinical study, elevation in the relative abundance of sphingomyelin and 1-stearoyl-2-docosahexaenoyl-GPC correlated with *Lactobacillus* depletion and genital

inflammation⁵¹. However, additional studies are needed in order to correlate elevated glycerolipids with cell death.

Early reports that dissect the metabolic potential of *Veillonella*^{49,63–66} revealed that *Veillonella* spp. utilize lactate as a sole energy source^{49,64,67}. Health-associated *Lactobacillus* spp. secrete copious amounts of lactic acid into the cervicovaginal milieu^{14,68,69} and lactic acid is depleted in severe cases of BV³. It is therefore possible that *V. atypica* and *V. montpellierensis* elicit their pathogenicity in the early stages of BV when lactate is still available. Our data support lactate utilization by *V. atypica* and *V. montpellierensis* (Fig. 5). Since current literature indicates lactate consumption by other *Megasphaera* spp.⁷⁰, our finding could be explained by suggesting that lactate serves as a non-primary energy source for *Megasphaera*. Importantly, we have shown that *Veillonella* spp. consume lactate (key metabolite associated with cervicovaginal health) and may contribute to changes in the cervicovaginal pH⁷¹. Indeed, in our previous clinical study investigating the vaginal microbiome in women across cervical neoplasia, *V. montpellierensis* and other *Veillonella* spp. were enriched in women with abnormal cervicovaginal pH³³.

Elevation of cervicovaginal polyamines is a metabolic hallmark of BV and contributes to increased pH and amine odor, both of which are key clinical symptoms of BV⁷². Polyamine synthesis by *Veillonella* has been documented in the oral microbiome and contributes to malodor⁷³. Additionally, one clinical study demonstrated that *M. micronuciformis* was associated with elevated cervicovaginal putrescine¹⁴. Our data revealed that in the context of our human 3-D cervical epithelial cell model, both *V. atypica* and *V. montpellierensis* modulate a variety of polyamines, including cadaverine, putrescine, histamine, and agmatine, whereas polyamines were not significantly elevated by *M. micronuciformis* infection (Fig. 5). Additionally, in previous clinical studies the metabolite 5'-methylthioadenosine (MTA), a by-product of polyamine synthesis, has been found to be depleted in women harboring non-*Lactobacillus* dominant microbiomes^{72,74,75}. In our current study, MTA was also depleted in *V. atypica* and *V. montpellierensis* infections. An earlier study¹⁴ provided clinical correlations for putrescine production by *Megasphaera* in a vaginal context, which is not in accordance with our data; however, the next-generation sequencing method employed was unable to identify *Megasphaera* at the species level. It is possible that other *Megasphaera* spp. present in the cervicovaginal microbiome may exert differential metabolic capabilities that influenced the observed elevation of putrescine in this study¹⁴. However, both the increase in polyamine synthesis and depletion of MTA observed in infections with *V. atypica* and *V. montpellierensis* suggest that these microorganisms may significantly impact polyamine synthesis in vivo and influence metabolic hallmarks of BV (e.g., putrescine and cadaverine).

Our data also revealed arginine depletion following *M. micronuciformis* infection. Nitric oxide, agmatine, and ornithine are by-products of arginine catabolism^{5,76}. Considering neither agmatine nor ornithine was significantly altered in our analysis, perhaps the observed depletion of arginine was a result of nitric oxide production by 3-D cervical cells. Nitric oxide has been implicated as an important toxic defense molecule against pathogens⁷⁷ and has a role in inflammation and the immune response, further indicating pro-inflammatory properties of *M. micronuciformis* in the cervicovaginal microenvironment⁷⁸.

In summary, lactate depletion and polyamine production observed in our 3-D human cervical cell model suggest that *Veillonella* spp. contribute to elevated cervicovaginal pH via consumption of a key metabolite linked to gynecologic health (Fig. 6). We found that *M. micronuciformis* exhibited greater pro-inflammatory properties compared to *V. atypica* and *V. montpellierensis*. *M. micronuciformis* infections also resulted in higher levels of epithelial cytotoxicity and a higher enrichment in SCFAs that can also impact the production of pro-inflammatory cytokines and

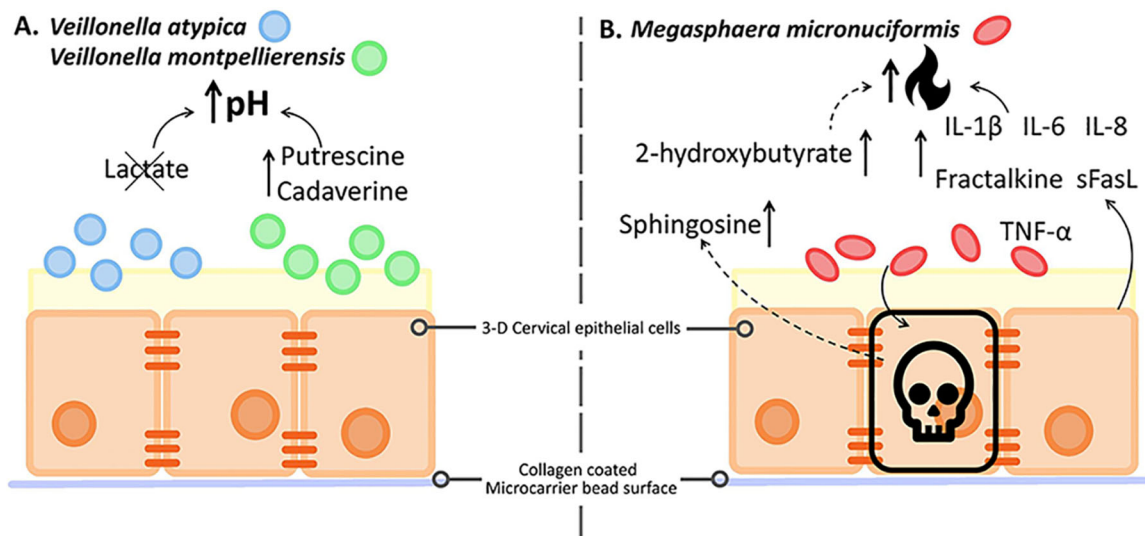


Fig. 6 Members of the Veillonellaceae family uniquely modify the immunometabolic cervical microenvironment. Summary of immunoproteomics and metabolomics analyses of 3-D cervical cells infected with *V. atypica*, *V. montpellierensis* or *M. micronuciformis*. **A** Lactate was depleted and polyamines (putrescine and cadaverine) are significantly accumulated in cell culture supernatants of 3-D cervical cells infected with either *V. atypica* or *V. montpellierensis*. Lactate (metabolic hallmark of cervicovaginal health) depletion and elevated polyamine levels may correspond with an increase in pH, a clinical hallmark of BV. **B** The SCFA 2-hydroxybutyrate was significantly accumulated in the cell culture supernatants of 3-D cervical cells infected with *M. micronuciformis*. In addition, several pro-inflammatory mediators were elevated following infection with *M. micronuciformis*, including IL-1 β , IL-6, IL-8, Fractalkine, sFasL, TNF- α . Finally, cytotoxicity/viability analyses revealed that *M. micronuciformis* infection resulted in moderate cervical epithelial cell death, as well as enrichment of sphingosine that could suggest the induction of cell death. Overall, *M. micronuciformis* may promote a pro-inflammatory immune profile within the cervical microenvironment, and cause cervical epithelial cell damage, compared to both *Veillonella* spp.

chemokines or cell death (Fig. 6). In line with our working hypothesis, our results provide evidence that *Veillonellaceae* family members alter the local microenvironment in a distinctive fashion. As putative primary colonizers, *Veillonella* spp. may create a favorable environment for secondary colonizers. On the other hand, *M. micronuciformis* may participate as a putative secondary colonizer that induces inflammation in the cervicovaginal tract and manifest as symptoms and clinical presentation of BV, as well as other gynecologic and reproductive sequelae (Fig. 6).

All experimental model systems have their own strengths and weaknesses⁷⁹. We acknowledge the polymicrobial nature of BV and inter-bacterial and host-microbe interactions that participate in the development and progression of the disease. In this study, we used a reductionist approach and performed mono-infections using our robust 3-D cervical cell model to dissect the individual contributions of specific *Veillonellaceae* members. This approach is required to first understand individual pathologic contributions from these understudied bacteria. This data will provide the foundations for future studies that utilize polymicrobial cocktails that better represent the complexity and microbe-microbe interactions present in the microbiome. Finally, our untargeted metabolomics approach is beneficial since it allows us to examine metabolic changes on a global scale. This technique is limited, however, by the relativistic nature of metabolite measurements and is therefore unable to provide absolute metabolite quantification. Future studies employing targeted metabolomics will help to directly compare concentrations of key cervicovaginal metabolites within in vivo samples and in vitro models.

Future studies on *Veillonellaceae* members in the context of the cervicovaginal epithelium should focus on the temporal colonization patterns of BV-associated organisms, as this will provide insights into the potential contribution to biofilm formation for these microorganisms. In addition, studies of polymicrobial “cocktails” that combine *Veillonellaceae* members with other vaginal bacterial isolates will provide additional insights into bacteria-bacteria interactions in the context of the cervicovaginal

microenvironment. In conclusion, the unique mechanisms and individual contributions of *Veillonellaceae* family members defined herein may promote our understanding of biofilm formation characteristic of BV and the underlying mechanisms that contribute to adverse obstetric/gynecologic health outcomes related to BV.

METHODS

Human cervical epithelial cell monolayer and three-dimensional human cervical cell model culture

Human cervical epithelial cells (A2EN) were grown as monolayers with keratinocyte serum-free media (Fischer Scientific) supplemented with endothelial growth factor (5 ng/ml), bovine pituitary extract (50 μ g/ml), and Primocin (100 μ g/ml) in the humidified atmosphere of 5% CO₂ at 37 °C⁴⁶. Primocin was not included in the media used in the bacterial infection assays outlined below. For 2-D monolayer cultures, cells were seeded into culture-treated 24-well plates to a cell density of $\sim 2 \times 10^5$ cells/ml. Prior to seeding, cells were enumerated using the Countess automated cell counter (Invitrogen) and trypan blue exclusion, which were used for cytotoxicity assays.

To generate the 3-D cervical cell model, human cervical epithelial A2EN cells were grown on Cytodex-3[®] collagen-coated dextran microcarrier beads (Sigma-Aldrich) in a rotating wall vessel bioreactor (Synthecon), as previously described^{15,45,46,80}. Following the 28-day differentiation period, aggregates were seeded into 24-well culture-treated plates at the density of 1×10^5 – 5×10^5 cells/ml and used for downstream analyses.

Bacterial strains and growth conditions

V. atypica strain CMW7756B and *V. montpellierensis* strain DNF00314 were cultured on brain heart infusion agar (Becton Dickinson) supplemented with 5% (v/v) defibrinated sheep blood (Quad Five) and 0.56 mg/l of sodium D-lactate (Sigma-Aldrich). *M. micronuciformis* strain DNF00954 was cultured on tryptic soy agar (Becton Dickinson) supplemented with 5% (v/v) defibrinated sheep blood (Quad Five). Bacteria were grown at 37 °C under anaerobic conditions generated using AnaeroPack sachets and anaerobic environmental chambers (Thermo Scientific). All strains were obtained from Biodefense and Emerging Infections Research Resources

Repository (<https://www.beiresources.org>). *M. micronuciformis* strain DNF00954 and *V. montpellierensis* strain DNF00314 were isolated from women with BV, whereas *V. atypica* strain CMW7756B was isolated from the genital tract of a pregnant woman.

Bacterial infection of human cervical epithelial cells

Prior to the infection, bacteria were grown for 16–18 h on appropriate agar plates, resuspended in sterile Dulbecco's phosphate-buffered saline (PBS), and adjusted to an optical density at 600 nm (OD_{600}) 0.5. The viability of bacteria was confirmed using the standard plating assay. The adjusted bacterial cell suspensions were serially diluted in PBS, plated on appropriate agar media, and incubated for 96 h at 37 °C under anaerobic conditions for enumeration of colony-forming units (CFU). The bacterial suspensions of OD_{600} 0.5 corresponded to bacterial densities of approximately $1-2 \times 10^8$ CFU/ml. Human cervical cell 2-D monolayers used for cytotoxicity assays were infected with a range of bacterial suspensions equivalent to OD_{600} of 0.001, 0.01, and 0.1 per 1×10^5 cervical cells/ml, which corresponded to multiplicities of infection (MOI) of 2–4, 20–40, and 200–400. Infected cervical cells were incubated for 24 h at 37 °C under anaerobic conditions. In a preliminary experiment, after 24 h incubation with cervical cells, the viability of bacteria was confirmed and did not change more than 1 log when compared to the initial inocula. The 3-D cervical epithelial cells were infected with the bacterial resuspensions at an MOI of 20–40 for 24 h at 37 °C under anaerobic conditions, as described above.

Lactate dehydrogenase (LDH) assay to assess cytotoxicity

The LDH assay (Invitrogen, ThermoFisher Scientific) was performed according to the manufacturer's guidelines. LDH activity was measured from cell culture supernatants by recording absorbance values at 490 and 680 nm. Spontaneous LDH activity was measured from PBS-treated cells and maximum LDH activity was measured from lysed cells. Percentage cytotoxicity was calculated by using the following formula: (bacteria-infected LDH activity – spontaneous LDH activity)/(the maximum LDH activity – spontaneous LDH activity) \times 100.

Scanning electron microscopy

Three-dimensional cervical epithelial cells were infected with each bacterial species at an MOI of 200–400 for 4 h at 37 °C under anaerobic conditions as described above. Samples were fixed and processed for scanning electron microscopy (SEM) as previously described^{80,81}. Samples were imaged using a JSM-6300 JEOL scanning electron microscope and images were obtained with the IXRF model 500 digital processor (IXRF systems). SEM images were pseudo-colored using Photoshop 19.0 CC (Adobe).

Immunoproteomic analysis of cell culture supernatants

Cell culture supernatants collected from at least three independent replicates of 3-D human cervical epithelial cells infected with bacteria as described above were used to quantify concentrations of 15 protein targets. PBS-treated cells served as negative controls. Cytometric bead arrays were performed using customized MILLIPLEX Multianalyte Profiling (MAP) Human Cytokine and Chemokine Panel 1, Human Circulating Cancer Panel 2, and Human Matrix Metalloproteinases Panel 2 (Millipore) in accordance with manufacturer guidelines. The tested targets included fractalkine, interleukin (IL)-1 α , IL-1 β , IL-6, IL-8, interferon- γ -induced protein-10 (IP-10), monocyte chemoattractant protein-1 (MCP-1), MCP-3, macrophage inflammatory protein-1 β (MIP-1 β), platelet-derived growth factor-AA (PDGF-AA), regulated on activation, normal T-cell expressed and secreted (RANTES), transforming growth factor- α (TGF- α), tumor necrosis factor- α (TNF- α), vascular endothelial growth factor (VEGF), macrophage migration inhibitory factor (MIF), tumor necrosis factor-related apoptosis-inducing ligand (TRAIL), soluble Fas ligand (sFasL), carcinoembryonic antigen (CEA), cancer antigen 125/mucin 16 (CA125), matrix metalloproteinase-1 (MMP-1), MMP-7, MMP-9, and MMP-10. Data was collected and analyzed using a Bio-Plex[®] 200 (Bio-Rad) platform and Bio-Plex[®] Manager (5.0) software (Bio-Rad). A 5-parameter logistic regression curve fit was used to determine concentrations. All reported values for MCP-1, MCP-3, MIP-1 β , and CA125 were below the minimum detectable concentration and were therefore not included in the further analyses. All samples were assayed in duplicate.

Untargeted global metabolomics analysis of cell culture supernatants

Cell culture supernatants collected from three independent 3-D cervical cell aggregate batches for both *Veillonella* strains and four independent batches for *M. micronuciformis* infections were sent to Metabolon Inc. (Durham, NC) for untargeted global metabolomics analysis. Metabolites were resolved on a Waters ACQUITY ultra-performance liquid chromatography (UPLC) and a Thermo Scientific Q-Exactive high resolution/accurate mass spectrometer interfaced with a heated electrospray ionization (HESI-II) source and Orbitrap mass analyzer operated at 35,000 mass resolution. The sample extract was dried then reconstituted in solvents compatible to each of the four methods. Each reconstitution solvent contained a series of standards at fixed concentrations to ensure injection and chromatographic consistency. One aliquot was analyzed using acidic positive ion conditions, chromatographically optimized for more hydrophilic compounds. In this method, the extract was gradient eluted from a C18 column (Waters UPLC BEH C18-2.1 \times 100 mm, 1.7 μ m) using water and methanol, containing 0.05% perfluoropentanoic acid (PFP) and 0.1% formic acid (FA). Another aliquot was also analyzed using acidic positive ion conditions; however, it was chromatographically optimized for more hydrophobic compounds. In this method, the extract was gradient eluted from the same aforementioned C18 column using methanol, acetonitrile, water, 0.05% PFP, and 0.01% FA and was operated at an overall higher organic content. Another aliquot was analyzed using basic negative ion optimized conditions using a separate dedicated C18 column. The basic extracts were gradient eluted from the column using methanol and water, however with 6.5 mM ammonium bicarbonate at pH 8. The fourth aliquot was analyzed via negative ionization following elution from a HILIC column (Waters UPLC BEH Amide 2.1 \times 150 mm, 1.7 μ m) using a gradient consisting of water and acetonitrile with 10 mM ammonium formate, pH 10.8. The MS analysis alternated between MS and data-dependent MSⁿ scans using dynamic exclusion. The scan range varied slightly between methods but covered 70–1000 *m/z*.

The bioinformatics system consisted of four major components, the Laboratory Information Management System (LIMS), the data extraction and peak-identification software, data processing tools for QC and compound identification, and a collection of information interpretation and visualization tools for use by data analysts. The hardware and software foundations for these informatics components were the LAN backbone, and a database server running Oracle 10.2.0.1 Enterprise Edition. Peaks were quantified using area-under-the-curve, which allows determining relative intensity of compounds among tested samples, but not the absolute concentrations.

Statistical analyses

All infections and assays were performed as at least three independent replicates. One-way ANOVA with Dunnett's adjustment for multiple comparisons was used to statistically analyze the immunoproteomics data. One-way ANOVA with Bonferroni post-hoc tests were used to test for significant differences in LDH data. Differences in metabolite pathway composition were determined by chi-squared analysis. One-way ANOVA analysis was performed using Prism v8 software (GraphPad). Hierarchical clustering analysis and heatmap visualization were performed using ClustVis⁸². Metabolite intensity values were median-scaled and log-transformed prior to performing two-tailed paired Student's *t*-tests (infection vs. PBS control) using the R *rstatix* package. Metaboanalyst 4.0⁸³ was used for principal component analysis (PCA), Pearson's correlation analysis, and metabolite pathway enrichment analysis. *P*-values of <0.05 were considered significant in all analyses. Metabolomics results were corrected for multiple testing using the false discovery rate (FDR) and *q*-values were reported. All error bars represent standard deviation.

Reporting summary

Further information on research design is available in the Nature Research Reporting Summary linked to this article.

DATA AVAILABILITY

The authors declare that the data supporting the findings of this study are available within the paper and its Supplementary Information files. Additional data are available from the corresponding author upon reasonable request.

Received: 12 December 2020; Accepted: 16 June 2021;
Published online: 06 July 2021

REFERENCES

- Berg, G. et al. Microbiome definition re-visited: old concepts and new challenges. *Microbiome* **8**, 103 (2020).
- Martin, D. H. & Marrazzo, J. M. The vaginal microbiome: current understanding and future directions. *J. Infect. Dis.* **214**, S36–S41 (2016).
- O'Hanlon, D. E., Moench, T. R. & Cone, R. A. In vaginal fluid, bacteria associated with bacterial vaginosis can be suppressed with lactic acid but not hydrogen peroxide. *BMC Infect. Dis.* **11**, 200 (2011).
- Muzny, C. A., Łaniewski, P., Schwebke, J. R. & Herbst-Kralovetz, M. M. Host-vaginal microbiota interactions in the pathogenesis of bacterial vaginosis. *Curr. Opin. Infect. Dis.* **33**, 59–65 (2020).
- Srinivasan, S. et al. Metabolic signatures of bacterial vaginosis. *MBio* **6**, <https://doi.org/10.1128/mBio.00204-15> (2015).
- Muzny, C. A. et al. An updated conceptual model on the pathogenesis of bacterial vaginosis. *J. Infect. Dis.* **220**, 1399–1405 (2019).
- Coudray, M. S. & Madhivanan, P. Bacterial vaginosis—a brief synopsis of the literature. *Eur. J. Obstet. Gynecol. Reprod. Biol.* **245**, 143–148 (2020).
- Kroon, S. J., Ravel, J. & Huston, W. M. Cervicovaginal microbiota, women's health, and reproductive outcomes. *Fertil. Steril.* **110**, 327–336 (2018).
- Ravel, J. & Brotman, R. M. Translating the vaginal microbiome: gaps and challenges. *Genome Med.* **8**, 35 (2016).
- Haahr, T. et al. Abnormal vaginal microbiota may be associated with poor reproductive outcomes: a prospective study in IVF patients. *Hum. Reprod.* **31**, 795–803 (2016).
- Menard, J. P. et al. High vaginal concentrations of *Atopobium vaginae* and *Gardnerella vaginalis* in women undergoing preterm labor. *Obstet. Gynecol.* **115**, 134–140 (2010).
- Łaniewski, P., İlhan, Z. E. & Herbst-Kralovetz, M. M. The microbiome and gynaecological cancer development, prevention and therapy. *Nat. Rev. Urol.* **17**, 232–250 (2020).
- Baker, J. M., Chase, D. M. & Herbst-Kralovetz, M. M. Uterine microbiota: residents, tourists, or invaders? *Front. Immunol.* **9**, 208 (2018).
- Ceccarani, C. et al. Diversity of vaginal microbiome and metabolome during genital infections. *Sci. Rep.* **9**, 14095 (2019).
- Gardner, J. K. et al. Interleukin-36γ is elevated in cervicovaginal epithelial cells in women with bacterial vaginosis and in vitro after infection with microbes associated with bacterial vaginosis. *J. Infect. Dis.* **221**, 983–988 (2020).
- Biagi, E. et al. Quantitative variations in the vaginal bacterial population associated with asymptomatic infections: a real-time polymerase chain reaction study. *Eur. J. Clin. Microbiol. Infect. Dis.* **28**, 281–285 (2009).
- Xia, Q. et al. Identification of vaginal bacteria diversity and its association with clinically diagnosed bacterial vaginosis by denaturing gradient gel electrophoresis and correspondence analysis. *Infect. Genet. Evol.* **44**, 479–486 (2016).
- Hughes, C. V., Roseberry, C. A. & Kolenbrander, P. E. Isolation and characterization of coaggregation-defective mutants of *Veillonella atypica*. *Arch. Oral Biol.* **35**, 1235–1255 (1990).
- Hussain, Q. A., McKay, I. J., Gonzales-Marin, C. & Allaker, R. P. Regulation of adrenomedullin and nitric oxide production by periodontal bacteria. *J. Periodontol Res* **50**, 650–657 (2015).
- Kolenbrander, P. E. Multispecies communities: interspecies interactions influence growth on saliva as sole nutritional source. *Int J. Oral Sci.* **3**, 49–54 (2011).
- Mitsui, T., Saito, M. & Harasawa, R. Salivary nitrate-nitrite conversion capacity after nitrate ingestion and incidence of *Veillonella* spp. in elderly individuals. *J. Oral Sci.* **60**, 405–410 (2018).
- Sato, T., Matsuyama, J., Sato, M. & Hoshino, E. Differentiation of *Veillonella atypica*, *Veillonella dispar* and *Veillonella parvula* using restricted fragment-length polymorphism analysis of 16S rDNA amplified by polymerase chain reaction. *Oral Microbiol. Immunol.* **12**, 350–353 (1997).
- Zhou, P., Liu, J., Merritt, J. & Qi, F. A YadA-like autotransporter, Hag1 in *Veillonella atypica* is a multivalent hemagglutinin involved in adherence to oral streptococci, *Porphyromonas gingivalis*, and human oral buccal cells. *Mol. Oral Microbiol.* **30**, 269–279 (2015).
- Zhou, P., Liu, J., Li, X., Takahashi, Y. & Qi, F. The sialic acid binding protein, Hsa, in *Streptococcus gordonii* DL1 also mediates intergeneric coaggregation with *Veillonella* species. *PLoS ONE* **10**, e0143898 (2015).
- Zhou, P., Li, X. & Qi, F. Identification and characterization of a haem biosynthesis locus in *Veillonella*. *Microbiology* **162**, 1735–1743 (2016).
- Roverly, C., Etienne, A., Foucault, C., Berger, P. & Brouqui, P. *Veillonella montpellierensis* endocarditis. *Emerg. Infect. Dis.* **11**, 1112–1114 (2005).
- Sillanpää, S. et al. Next-generation sequencing combined with specific PCR assays to determine the bacterial 16S rRNA gene profiles of middle ear fluid collected from children with acute otitis media. *mSphere* **2**, <https://doi.org/10.1128/mSphere.00006-17> (2017).
- Xu, J. et al. Microbial biomarkers of common tongue coatings in patients with gastric cancer. *Micro. Pathog.* **127**, 97–105 (2019).
- Zhao, Z. et al. Metagenome association study of the gut microbiome revealed biomarkers linked to chemotherapy outcomes in locally advanced and advanced lung cancer. *Thorac. Cancer* <https://doi.org/10.1111/1759-7714.13711> (2020).
- Belström, D. et al. Altered bacterial profiles in saliva from adults with caries lesions: a case-cohort study. *Caries Res.* **48**, 368–375 (2014).
- Fredricks, D. N., Fiedler, T. L. & Marrazzo, J. M. Molecular identification of bacteria associated with bacterial vaginosis. *N. Engl. J. Med.* **353**, 1899–1911 (2005).
- Ranjit, E., Raghubanshi, B. R., Maskey, S. & Parajuli, P. Prevalence of bacterial vaginosis and its association with risk factors among nonpregnant women: a hospital based study. *Int J. Microbiol.* **2018**, 8349601 (2018).
- Łaniewski, P. et al. Linking cervicovaginal immune signatures, HPV and microbiota composition in cervical carcinogenesis in non-Hispanic and Hispanic women. *Sci. Rep.* **8**, 7593 (2018).
- Wang, B. et al. Molecular analysis of the relationship between specific vaginal bacteria and bacterial vaginosis metronidazole therapy failure. *Eur. J. Clin. Microbiol. Infect. Dis.* **33**, 1749–1756 (2014).
- Marchandin, H. & Jumas-Bilak, E. The Family Veillonellaceae. The Prokaryotes: Firmicutes and Tenericutes. 433–453 (2014).
- Smith, W. L. et al. Cervical and vaginal flora specimens are highly concordant with respect to bacterial vaginosis-associated organisms and commensal *Lactobacillus* species in women of reproductive age. *J. Clin. Microbiol.* **52**, 3078–3081 (2014).
- Brusselsaers, N., Shrestha, S., van de Wijgert, J. & Verstraelen, H. Vaginal dysbiosis and the risk of human papillomavirus and cervical cancer: systematic review and meta-analysis. *Am. J. Obstet. Gynecol.* **221**, 9–18 (2019).
- Bautista, C. T. et al. Bacterial vaginosis: a synthesis of the literature on etiology, prevalence, risk factors, and relationship with chlamydia and gonorrhea infections. *Mil. Med. Res.* **3**, 4 (2016).
- Mitchell, C. et al. Interaction between lactobacilli, bacterial vaginosis-associated bacteria, and HIV Type 1 RNA and DNA genital shedding in U.S. and Kenyan women. *AIDS Res. Hum. Retroviruses* **29**, 13–19 (2013).
- Nelson, D. B. et al. Early pregnancy changes in bacterial vaginosis-associated bacteria and preterm delivery. *Paediatr. Perinat. Epidemiol.* **28**, 88–96 (2014).
- Hočevar, K. et al. Vaginal microbiome signature is associated with spontaneous preterm delivery. *Front. Med.* **6**, 201 (2019).
- Glascok, A. L. et al. Unique roles of vaginal *Megasphaera* phylotypes in reproductive health. Preprint at <https://www.biorxiv.org/content/10.1101/2020.08.18.246819v1.full> (2020).
- Yagihashi, Y. & Arakaki, Y. Acute pyelonephritis and secondary bacteraemia caused by *Veillonella* during pregnancy. *BMJ Case Rep.* <https://doi.org/10.1136/bcr-2012-007364> (2012).
- Jackson, R., Maarsingh, J. D., Herbst-Kralovetz, M. M. & Van Doorslaer, K. 3D oral and cervical tissue models for studying papillomavirus host-pathogen interactions. *Curr. Protoc. Microbiol.* **59**, e129 (2020).
- Radtke, A. L. & Herbst-Kralovetz, M. M. Culturing and applications of rotating wall vessel bioreactor derived 3D epithelial cell models. *J. Vis. Exp.* <https://doi.org/10.3791/3868> (2012).
- Radtke, A. L., Quayle, A. J. & Herbst-Kralovetz, M. M. Microbial products alter the expression of membrane-associated mucin and antimicrobial peptides in a three-dimensional human endocervical epithelial cell model. *Biol. Reprod.* **87**, 132 (2012).
- Barrila, J. et al. Organotypic 3D cell culture models: using the rotating wall vessel to study host-pathogen interactions. *Nat. Rev. Microbiol.* **8**, 791–801 (2010).
- Ohnishi, A. et al. Development of a 16S rRNA gene primer and PCR-restriction fragment length polymorphism method for rapid detection of members of the genus *Megasphaera* and species-level identification. *Appl. Environ. Microbiol.* **77**, 5533–5535 (2011).
- Rogosa, M. & Bishop, F. S. The genus *Veillonella*. II. Nutritional studies. *J. Bacteriol.* **87**, 574–580 (1964).
- Doerflinger, S. Y., Throop, A. L. & Herbst-Kralovetz, M. M. Bacteria in the vaginal microbiome alter the innate immune response and barrier properties of the human vaginal epithelia in a species-specific manner. *J. Infect. Dis.* **209**, 1989–1999 (2014).
- Ilhan, Z. E. et al. Deciphering the complex interplay between microbiota, HPV, inflammation and cancer through cervicovaginal metabolic profiling. *EBioMedicine* **44**, 675–690 (2019).
- Herbst-Kralovetz, M. M. et al. Quantification and comparison of toll-like receptor expression and responsiveness in primary and immortalized human female lower genital tract epithelia. *Am. J. Reprod. Immunol.* **59**, 212–224 (2008).
- Patterson, J. L., Stull-Lane, A., Girerd, P. H. & Jefferson, K. K. Analysis of adherence, biofilm formation and cytotoxicity suggests a greater virulence potential of

- Gardnerella vaginalis* relative to other bacterial-vaginosis-associated anaerobes. *Microbiology* **156**, 392–399 (2010).
54. van Teijlingen, N. H. et al. Vaginal dysbiosis associated-bacteria *Megasphaera elsdenii* and *Prevotella timonensis* induce immune activation via dendritic cells. *J. Reprod. Immunol.* **138**, 103085 (2020).
 55. Lennard, K. et al. Microbial composition predicts genital tract inflammation and persistent bacterial vaginosis in South African adolescent females. *Infect. Immun.* **86**, <https://doi.org/10.1128/IAI.00410-17> (2018).
 56. Aldunate, M. et al. Antimicrobial and immune modulatory effects of lactic acid and short chain fatty acids produced by vaginal microbiota associated with eubiosis and bacterial vaginosis. *Front. Physiol.* **6**, 164 (2015).
 57. Delgado-Diaz, D. J. et al. Distinct immune responses elicited from cervicovaginal epithelial cells by lactic acid and short chain fatty acids associated with optimal and non-optimal vaginal microbiota. *Front. Cell Infect. Microbiol.* **9**, 446 (2019).
 58. Mirmonsef, P. et al. Short-chain fatty acids induce pro-inflammatory cytokine production alone and in combination with toll-like receptor ligands. *Am. J. Reprod. Immunol.* **67**, 391–400 (2012).
 59. Matera, G. et al. Receptor recognition of and immune intracellular pathways for *Veillonella parvula* lipopolysaccharide. *Clin. Vaccin. Immunol.* **16**, 1804–1809 (2009).
 60. Maceyka, M. & Spiegel, S. Sphingolipid metabolites in inflammatory disease. *Nature* **510**, 58–67 (2014).
 61. Ibrinke, O. et al. Species-level evaluation of the human respiratory microbiome. *Gigascience* **9**, <https://doi.org/10.1093/gigascience/giaa038> (2020).
 62. Morales, A., Lee, H., Goñi, F. M., Kolesnick, R. & Fernandez-Checa, J. C. Sphingolipids and cell death. *Apoptosis* **12**, 923–939 (2007).
 63. Rogosa, M. & Bishop, F. S. The genus *Veillonella*. 3. Hydrogen sulfide production by growing cultures. *J. Bacteriol.* **88**, 37–41 (1964).
 64. Rogosa, M. The genus *Veillonella*. I. General cultural, ecological, and biochemical considerations. *J. Bacteriol.* **87**, 162–170 (1964).
 65. Rogosa, M. The genus *Veillonella* IV. Serological groupings, and genus and species emendations. *J. Bacteriol.* **90**, 704–709 (1965).
 66. Rogosa, M., Krichevsky, M. I. & Bishop, F. S. Truncated glycolytic system in *Veillonella*. *J. Bacteriol.* **90**, 164–171 (1965).
 67. Jurtschuk Jr, P. & Baron, S. Medical Microbiology. 4th Edn. Galveston (TX): University of Texas medical branch at Galveston. *Bacterial Metabolism*. Chapter 4 (1996).
 68. Mirmonsef, P. et al. The effects of commensal bacteria on innate immune responses in the female genital tract. *Am. J. Reprod. Immunol.* **65**, 190–195 (2011).
 69. Sobel, J. D. Is there a protective role for vaginal flora? *Curr. Infect. Dis. Rep.* **1**, 379–383 (1999).
 70. Shetty, S. A., Marathe, N. P., Lanjekar, V., Ranade, D. & Shouche, Y. S. Comparative genome analysis of *Megasphaera* sp. reveals niche specialization and its potential role in the human gut. *PLoS ONE* **8**, e79353 (2013).
 71. Boskey, E. R., Cone, R. A., Whaley, K. J. & Moench, T. R. Origins of vaginal acidity: high D/L lactate ratio is consistent with bacteria being the primary source. *Hum. Reprod.* **16**, 1809–1813 (2001).
 72. Nelson, T. M. et al. Vaginal biogenic amines: biomarkers of bacterial vaginosis or precursors to vaginal dysbiosis? *Front. Physiol.* **6**, 253 (2015).
 73. Al-Hebshi, N. N. et al. Metagenome sequencing-based strain-level and functional characterization of supragingival microbiome associated with dental caries in children. *J. Oral. Microbiol.* **11**, 1557986 (2019).
 74. Evans, G. B., Furneaux, R. H., Schramm, V. L., Singh, V. & Tyler, P. C. Targeting the polyamine pathway with transition-state analogue inhibitors of 5'-methylthioadenosine phosphorylase. *J. Med. Chem.* **47**, 3275–3281 (2004).
 75. Kamatani, N. & Carson, D. A. Abnormal regulation of methylthioadenosine and polyamine metabolism in methylthioadenosine phosphorylase-deficient human leukemic cell lines. *Cancer Res.* **40**, 4178–4182 (1980).
 76. Mori, M. & Gotoh, T. Regulation of nitric oxide production by arginine metabolic enzymes. *Biochem. Biophys. Res. Commun.* **275**, 715–719 (2000).
 77. Tripathi, P. Nitric oxide and immune response. *Indian J. Biochem. Biophys.* **44**, 310–319 (2007).
 78. Moilanen, E. & Vapaatalo, H. Nitric oxide in inflammation and immune response. *Ann. Med.* **27**, 359–367 (1995).
 79. Herbst-Kralovetz, M. M., Pyles, R. B., Ratner, A. J., Sycuro, L. K. & Mitchell, C. New systems for studying intercellular interactions in bacterial vaginosis. *J. Infect. Dis.* **214**, S6–S13 (2016).
 80. McGowan, C. L., Radtke, A. L., Abraham, K., Martin, D. H. & Herbst-Kralovetz, M. *Mycoplasma genitalium* infection activates cellular host defense and inflammation pathways in a 3-dimensional human endocervical epithelial cell model. *J. Infect. Dis.* **207**, 1857–1868 (2013).
 81. Hjelm, B. E., Berta, A. N., Nickerson, C. A., Arntzen, C. J. & Herbst-Kralovetz, M. M. Development and characterization of a three-dimensional organotypic human vaginal epithelial cell model. *Biol. Reprod.* **82**, 617–627 (2010).
 82. Jaak, M., Jaak, T. & Jaak, V. Clustvis: a web tool for visualizing clustering of multivariate data using Principal Component Analysis and heatmap. *Nucleic Acids Res.* **43**, W566–W570 (2015).
 83. Chong, J., Wishart, D. S. & Xia, J. Using MetaboAnalyst 4.0 for comprehensive and integrative metabolomics data analysis. *Curr. Protoc. Bioinformatics* **68**, e86 (2019).

ACKNOWLEDGEMENTS

We thank David Lowry at Arizona State University for his aid in SEM sample preparation and imaging. In addition, we are thankful to Dr. Zehra Esra Ilhan for critically reviewing the manuscript. Also, we would like to acknowledge the Biodefense and Emerging Infections Research Resources Repository (<https://www.beiresearch.org>), NIAID, NIH as a part of the Human Microbiome Project for supplying bacterial isolates for this study; *V. atypica* strain CMW7756B, *V. montpellierensis* strain DNF00314 and *M. micronuciformis* strain DNF00954. Funding for this project was provided by the NIH National Cancer Institute and a supplement from the Office of Research for Women's Health (3P30CA023074-3953) and the Flinn Foundation Grant# 2244.

AUTHOR CONTRIBUTIONS

M.M.H.-K. conceived of the hypothesis and experimental design in collaboration with J.D.M. and P.L. M.E.S. carried out 3-D cervical cell infections used in immunometabolomics analysis, wrote the first draft of the manuscript, drafted and edited the figures, and revised the manuscript. J.D.M. obtained SEM images of infected 3-D cervical cells and assisted in statistical analysis. C.G. performed LDH and crystal violet assays, analysis of LDH data, and presentation of LDH figures, as well as revision of the manuscript. M.M.H.-K., J.D.M., and P.L. provided guidance and feedback on writing, figures and tables, and read and revised the manuscript. M.M.H.-K. provided supervision of the experimental and writing processes. All authors read, revised, and approved the final version of the manuscript.

COMPETING INTERESTS

The authors declare no competing interests.

ADDITIONAL INFORMATION

Supplementary information The online version contains supplementary material available at <https://doi.org/10.1038/s41522-021-00229-0>.

Correspondence and requests for materials should be addressed to M.M.H.-K.

Reprints and permission information is available at <http://www.nature.com/reprints>

Publisher's note Springer Nature remains neutral with regard to jurisdictional claims in published maps and institutional affiliations.



Open Access This article is licensed under a Creative Commons Attribution 4.0 International License, which permits use, sharing, adaptation, distribution and reproduction in any medium or format, as long as you give appropriate credit to the original author(s) and the source, provide a link to the Creative Commons license, and indicate if changes were made. The images or other third party material in this article are included in the article's Creative Commons license, unless indicated otherwise in a credit line to the material. If material is not included in the article's Creative Commons license and your intended use is not permitted by statutory regulation or exceeds the permitted use, you will need to obtain permission directly from the copyright holder. To view a copy of this license, visit <http://creativecommons.org/licenses/by/4.0/>.

© The Author(s) 2021